

Study of interaction of hypericin and its pharmaceutical preparation by fluorescence techniques

Jun Liu

National University of Singapore
Department of Chemistry
3 Science Drive 3
Singapore 117543, Singapore

and
National University of Singapore
Graduate Programme in Bioengineering
#05-01 Centre for Life Sciences
28 Medical Drive
Singapore 117456, Singapore

Constance Lay Lay Saw*

National University of Singapore
Department of Pharmacy
18 Science Drive 4
Singapore 117543, Singapore

and
National Cancer Centre Singapore
Division of Medical Sciences
11 Hospital Drive
Singapore 169610, Singapore

Malini Olivo

National University of Singapore
Department of Pharmacy
18 Science Drive 4
Singapore 117543, Singapore

and
National Cancer Centre Singapore
Division of Medical Sciences
11 Hospital Drive
Singapore 169610, Singapore

and
Singapore Bioimaging Consortium
Bio-optical Imaging
11 Biopolis Street #02-02 Helios
Singapore 138667, Singapore

Thankiah Sudhaharan

Sohail Ahmed

Institute of Medical Biology Singapore
8A Medical Grove
Singapore 138665, Singapore

Paul Wan Sia Heng

National University of Singapore
Department of Pharmacy
18 Science Drive 4
Singapore 117543, Singapore

Thorsten Wohland

National University of Singapore
Department of Chemistry
3 Science Drive 3
Singapore 117543, Singapore

Abstract. We report the detection of interactions between a photosensitizer, hypericin (HY), and its solvent system prepared with a formulation additive, polyvinylpyrrolidone (PVP), a commonly used pharmaceutical excipient. Fluorescence correlation spectroscopy (FCS) and fluorescence lifetime imaging microscopy (FLIM) were used to study aggregation and binding of HY in the presence of PVP. Digitized fluorescence endoscopic imaging (DFEI) was used to study the effect of the pharmaceutical formulation in the *in vivo* tumor implanted chick chorioallantoic membrane (CAM) model. The results presented reveal the coordination of HY-PVP binding, HY disaggregation in the presence of PVP, and strengthened HY tumor uptake selectivity. PVP is thus suggested as a potential adjuvant to previously investigated N-methyl pyrrolidone (NMP) in the HY delivery system as well as a replacement for the conventionally used albumin in the HY bladder instillation fluids preparation for clinical use. © 2009 Society of Photo-Optical Instrumentation Engineers. [DOI: 10.1117/1.3067726]

Keywords: hypericin (HY); N-methyl pyrrolidone (NMP); polyvinylpyrrolidone (PVP); fluorescence correlation spectroscopy (FCS); fluorescence lifetime imaging microscopy (FLIM); digitized fluorescence endoscopic imaging (DFEI); chick chorioallantoic membrane (CAM); photodynamic therapy and diagnosis; drug delivery.

Paper 08275R received Aug. 8, 2008; revised manuscript received Nov. 4, 2008; accepted for publication Nov. 13, 2008; published online Jan. 21, 2009.

1 Introduction

Fluorescence correlation spectroscopy (FCS) is a method to study molecular movement and concentration with single-molecule sensitivity. Fluctuations in the fluorescence signal from fluorophores in an illuminated focal volume provide information about molecular dynamics via autocorrelation analysis.¹ FCS has many applications in life sciences, where it is a routine tool for the study of biomolecular diffusion and interactions.²⁻⁶ Many pharmaceutical companies have exploited its miniaturized high-throughput screening capability in discovering potential lead compounds for drug discovery,⁷⁻⁹ and FCS has been employed in drug delivery system characterization.¹⁰ Fluorescence lifetime imaging microscopy (FLIM) measures the fluorescence lifetime at each pixel within an image of a sample. It has been commonly used to distinguish among different types of fluorophores, the state of the fluorophore (e.g., aggregated versus nonaggregated, or protonated versus deprotonated states), and the fluorophore environment.¹¹⁻¹⁷ HY fluorescence lifetimes in different sol-

*Present address: Rutgers The State University of New Jersey, Department of Pharmaceutics, Ernest Mario School of Pharmacy, 160 Frelinghuysen Road, Piscataway, NJ 08854.

Address all correspondence to: Thorsten Wohland, National University of Singapore, Department of Chemistry, 3 Science Drive 3, Singapore 117543, Singapore. Tel: +65 6516 1248; Fax: +65 6779 1691; E-mail: chmw@nus.edu.sg.

vents have been reported,^{18–20} and FLIM measurements in retinal pigment epithelium cells have revealed the influence of HY self-quenching in its fluorescence lifetime.²¹ The present study attempts to identify with FCS and FLIM the interactions among hypericin (HY), a promising photosensitizer, a novel pharmaceutical preparation containing N-methyl pyrrolidone (NMP), a penetration enhancer, and polyvinylpyrrolidone (PVP), a commonly used pharmaceutical excipient, for photodynamic applications such as photodynamic therapy (PDT) and photodynamic diagnosis (PDD) of cancers. PDT is a modality of cancer treatment that uses light-induced activity of a photosensitizer to treat cancer. It has been proven to be beneficial for several superficial cancers.²² PDD uses light-induced fluorescence of a photosensitizer to detect cancer. There have been reports that such detection methods provide significant improvement compared to the gold standard of white-light inspection by trained clinicians, in terms of sensitivity and specificity.^{23,24}

The potential use of NMP for formulation of photosensitizers including HY has been reported.^{25–28} Comparison with the current clinically used HY–human serum albumin (HSA) formulation has shown the potential use of NMP in improving the cancer detecting ability and photodynamic therapeutic effects of HY and shortening the administration time of HY formulation when used clinically.^{28,29}

In order to improve on the water insolubility of HY, one of its major drawbacks, a water-soluble derivative of HY has been produced and reported to possess a higher cellular uptake level as well as higher phototoxicity than the nonsoluble HY.³⁰ However, another approach to improve solubility and delivery of HY by preparing liposomes was found with no effect on the binding and transport of HY in the Caco-2 cells model.³¹ Plasma protein was proposed as an “effective” HY transporter/carrier increasing the water solubility of HY.²⁴ However, it was reported that the 2 h exposure of the cells to HY in the absence of serum resulted in the highest intracellular accumulation of HY³² and that HY is tightly bound to HSA.³³ When HY-HSA bladder instillation fluid is to be used clinically, this might lead to a slow release of HY. Recently, different approaches to delivery of HY with contrasting findings were reviewed.³⁴ Thus, in the development of a pharmaceutical formulation for HY, two issues need to be addressed: Does any interaction exist between HY and the solvent system? And if so, at what concentration of the pharmaceutical excipients will such interaction occur? In order to answer these questions, we report the use of FCS and FLIM to study pharmaceutical preparations and to effectively determine the suitable amounts of PVP that should be used for further investigation of different formulations of HY, followed by *in vivo* assessment with digitized fluorescence endoscopic imaging (DFEI) on chick chorioallantoic membrane (CAM) implanted with tumor cells. The DFEI of CAMs was a simple and rapid step to assess the FCS results while at the same time setting up a reference for further endoscopic studies of PVP as a regular excipient for HY used on other animal models and eventually patients (e.g., PDD for bladder and oral cancers).

Table 1 Characteristics of the spectrally similar fluorophores used.

	Hypericin	Atto 565
Molecular weight	504.45	547.04
Absorption wavelength	556 nm	565 nm
Emission wavelength	592 nm	590 nm

2 Materials and Methods

2.1 Materials

Hypericin (HY) was purchased from Molecular Probes (Eugene, Oregon) N-methyl pyrrolidone (NMP, Pharmasolve), polyvinylpyrrolidone (PVP, Plasdone K29/32, C15), and vinylpyrrolidone-vinylacetate 60:40 copolymer copolyvidonum (Plasdone S630) were kindly supplied by International Specialty Products (Wayne, New York) Phosphate buffer solution (PBS, pH 7.4) was the bulk medium used in the HY formulation. Atto 565, fluorescein isothiocyanate (FITC) and dimethyl sulfoxide (DMSO) were purchased from Fluka, Sigma-Aldrich (Singapore).

2.2 Instrumentation, Measurements, and Analysis

2.2.1 FCS analysis on HY solutions

FCS measurements were performed on an inverted confocal microscope (FV300, Olympus, Singapore). The setup³⁵ consists of a HeNe ion laser (Melles Griot, Singapore) which provides an excitation beam at a wavelength set at 543 nm and a power of 90 μ W. The beam is then reflected by a dichroic mirror, 560 DRLP (Omega Optical, Brattleboro, Vermont), before being focused by an objective into a focal volume as small as about 0.2 to 0.3 μ m in radius and 1.0 to 1.5 μ m in height. The fluorescence emitted from the sample was collected by the same objective and then transmitted through the same dichroic mirror and a 550 to 600-nm bandpass filter before finally being directed to the detector. The autocorrelation curves of the detected intensity signal from an external hardware correlator (Flex02-12D, correlator.com, Zhejiang, China) were fitted with a self-written program in IgorPro (Wavemetrics, Inc., Lake Oswego, Oregon).

All measurements were carried out in PBS, pH 7.4. To verify the nonexistence of interaction between HY and NMP, an 80- μ L drop of 1-nM HY solution with cascading concentrations of NMP was deposited on a 0.17-mm microscope coverslip for measurement in the microscope. Following this, solution samples containing 5-mM NMP (approximately 0.05% v/v, a biocompatible concentration determined *in vivo*²⁶), 10-nM HY (a fixed concentration experimentally selected from a series, with optimum signal intensity within the effective range of FCS measurement), and various concentrations between 10 μ M and 10 mM of PVP K29/32, PVP C15, or S630 were used. Atto 565, a fluorophore with a molecular weight as well as excitation and emission wavelength close to HY, was used as a standard and control in similar experiments (Table 1). We have no evidence that Atto565 interacts with the polymers at the used concentrations, and it is thus assumed to

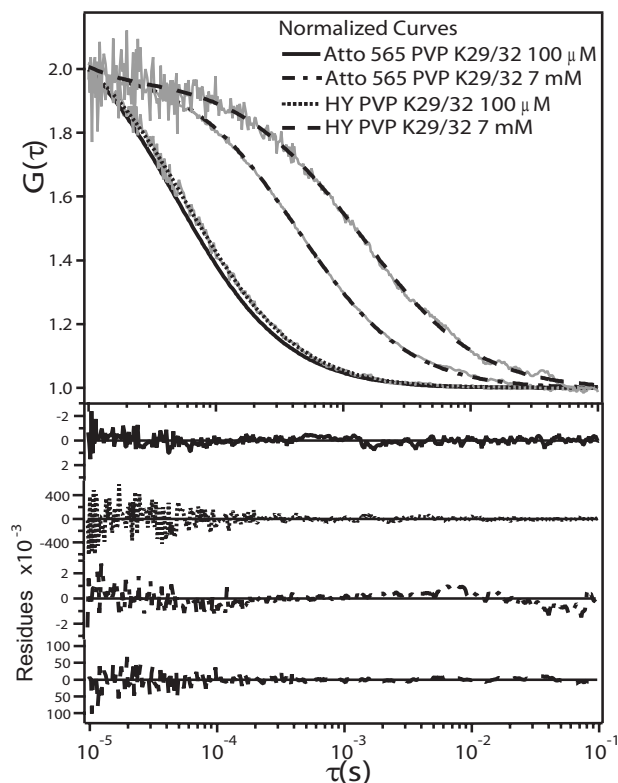


Fig. 1 Fitting for autocorrelation curves with residues and their widening due to increasing viscosity (black for Atto 565 and blue for HY) and particle interactions with PVP (solid line for PVP 100 μM and dotted line for PVP 7 mM).

be a good probe to test viscosity and refractive index of the used solutions. At least 15 independent measurements were conducted for each concentration in every set of experiments for statistical reliability, and each set of experiments was independently repeated at least three times for reproducibility.

Autocorrelation curves $G(\tau)$ obtained from the fluorescence intensity signals sent to the hardware correlator (Fig. 1) were fitted using either the 3-D one-particle [Eq. (1)] or the 3-D two-particle [Eq. (2)] diffusion model,^{36,37} the selection of which depended on the quality of fitting:

$$G(\tau) = \frac{1}{N} \left(1 + \frac{\tau}{\tau_D}\right)^{-1} \left(1 + \frac{\tau}{\tau_D K^2}\right)^{-0.5} + G_\infty, \quad (1)$$

$$G(\tau) = \frac{1}{N} \left[F_2 \left(1 + \frac{\tau}{\tau_D}\right)^{-1} \left(1 + \frac{\tau}{\tau_D K^2}\right)^{-0.5} + (1 - F_2) \left(1 + \frac{\tau}{\tau_{D_2}}\right)^{-1} \left(1 + \frac{\tau}{\tau_{D_2} K^2}\right)^{-0.5} \right] + G_\infty. \quad (2)$$

In Eq. (1), N is the average number of particles within the focal volume; τ_D is the diffusion time of the particle; K is the structure factor of the focal volume, given by the ratio of the length to the width of the focal volume, determined from calibration measurements. G_∞ is the convergence value for the autocorrelation curve for long times, expected to be 1. It is

kept as a free parameter to improve fitting but differs by less than 3% from 1 in all cases. In Eq. (2), F_2 is the bound fraction, i.e., ratio of number of bound particles over total number of particles; τ_{D_2} is the diffusion time of the second particle; and the other parameters are defined following Eq. (1). When Eq. (2) is used for fitting, τ_D is fixed to viscosity and molecular weight corrected values calculated from Atto 565 measurements.

The average numbers of HY and Atto 565 particles (N_{HY} and $N_{\text{Atto 565}}$, respectively) within the focal volume were obtained from statistics of fitted autocorrelation functions from each measurement. Increasing concentrations of PVP lead to changes in the refractive index of the solution, and the focal volume will increase with the refractive index since this increases the mismatch between the immersion medium (water) and the mounting medium (PVP solutions).³⁸ In order to remove the effect of changing refractive index in solutions with various concentration of PVP represented by the changing $N_{\text{Atto 565}}$, the relative ratio of average number of particles R_N is defined as follows:

$$R_N = \frac{N_{\text{HY}}}{N_{\text{Atto 565}}}. \quad (3)$$

2.2.2 FLIM analysis on HY solutions

The FLIM measurements were performed with a LIFA system (Lambert Instruments, Roden, The Netherlands) on an inverted wide-field fluorescence microscope (Olympus IX81, Center Valley, Pennsylvania) with an Olympus PlanApoN 60X/1.45 oil immersion objective and a filter set XF108-2 (Omega Optical, Brattleboro, Vermont) consisting of an excitation filter 525AF45, a dichroic mirror 560 DRLP, and an emission filter 595AF60. Fluorescence lifetime of HY was measured using the frequency domain method. The average lifetime from each measurement was determined by software (LI-FLIM) supplied by the manufacturer. The excitation source was a 4-mW, 470-nm phase-modulated LED. FITC was used as a lifetime reference with a set lifetime of 4 ns. All measurements were carried out in PBS, pH 7.4. Solution samples containing 5-mM NMP, 100- μM HY, and concentrations between 10 μM and 10 mM of PVP K29/32, PVP C15, or S630 were used for fluorescence lifetime measurements. In order to reveal the possible influence of change in hydrophobicity of the environment on the HY lifetime, the same set of measurements were performed on DMSO solutions at concentrations equivalent to those of monomerized PVP 29/32 units in its corresponding concentrations. At least three independent measurements were conducted for each concentration in every set of experiments for statistical reliability, and each set of experiments was independently repeated at least two times for reproducibility.

2.2.3 DFEI on tumor-implanted CAM

In order to perform an assessment of the FCS results, CAM was used as a viable and economic *in vivo* model for tumor transplantation and fluorescence endoscopic imaging.

CAM was prepared following the same method as previously reported.²⁵ Fertilized chicken eggs were disinfected with 70% ethanol and placed on trays with the blunt end

facing upward. They were then incubated for 7 days in an egg incubator (Octagon 20, Brinsea, Somerset, UK) at 37.4 °C with 60% humidity and occasional turnings. On day 7 of embryo age (EA 7), a window was opened at the apex of the egg to create a false air sac, and the opening was then covered with parafilm. On the next day after opening, 5×10^6 human bladder carcinoma cells (MGH) were transplanted on each CAM, prepared following the method reported previously.³⁹ The eggs were then incubated in the same environment without turnings until EA 14, when they were mature and ready for experiments.⁴⁰

On EA 14, 1-mL HY solution was instilled to cover the whole surface area of the CAM. The window was covered with parafilm to prevent evaporation of solution and incubated in the absence of light. The remaining solution was then removed from the CAM surface with the aid of micropipettes. Each surface was washed three times with 1-mL 0.9% w/v NaCl solution to remove excess photosensitizer. The CAM with implanted tumor was then immediately used for fluorescence endoscopic imaging.

In all experiments, the NMP concentration was fixed to 500 μM (about 0.005% v/v), a concentration reported to be harmless to normal CAM membranes.²⁶ Extensive preliminary experiments were carried out in order to identify the dose of HY (1- μM to 100- μM HY) and incubation time for the uptake of HY into tumor cells implanted in CAM to occur (15, 30, 45, 60, and 180 min) for optimum photodynamic diagnostic efficiency. Since 10- μM HY solutions produced results distinguishable enough after 1-h incubation, subsequent quantitative studies were carried out with 10- μM HY solutions with different PVP K29/32 concentrations (0 μM , 100 μM , 1 mM, 5 mM, and 10 mM), and fluorescence endoscopic images were taken after 1-h incubation for photodynamic diagnostics and 3-h incubation as an endpoint for comparing rates at which HY was removed from tissues (referred to as the “clearance” in the rest of this paper). The same treatment with non-HY solutions were carried out on 6 to 10 eggs for each PVP concentration group (each group was equally subdivided as tumor-implanted and non-tumor-implanted subgroups, i.e., 3 to 5 eggs for each subgroup) as a control.

The developed DFEI system has been reported in detail.⁴¹ The DFEI system mainly consists of an illumination console, a fluorescence detection unit, and a computing system for image acquisition, display, and processing. A 100-W xenon short arc lamp (D-Light AF system, Karl Storz, Tuttlingen, Germany) was used for *in vivo* tissue fluorescence excitation (370 to 450 nm, approximately 50 mW at the endoscope tip) and white light illumination. Both illumination and observation of tissues of interest were achieved via a modified endoscope with an integrated long-pass filter (cutoff wavelength at 560 nm). Image detection was performed with a three-chip color CCD video camera (Tircam SL PDD, Karl Storz, Tuttlingen, Germany). The RGB video outputs of the camera were fed to a frame grabber (Matrox Genesis-LC, Dorval, Quebec, Canada) for image capturing and digitizing.

During fluorescence image data processing, the ratio (I_R/I_B) of the red HY fluorescence intensity (I_R) over the blue backscattered excitation intensity (I_B) was applied as a ratio diagnostic algorithm. The reason for using I_R/I_B rather than

the simple representation of fluorescence intensity by I_R is that both the fluorescence intensity and the intensity of the remitted blue light depend similarly upon the distance between the detected surface and the detection unit, the angles of the irradiation and observation, and the tissue optical properties, as demonstrated in bladder cancer detection by Zaak et al.⁴² In order to further demonstrate the effect of PVP K29/32 (representative of the three polymers tested with FCS) in HY delivery and its selective uptake by tumor cells, the ratio of I_R/I_B from tumor over I_R/I_B from normal tissue (CAM) was calculated and defined as the selectivity index I_S :

$$I_S = \frac{I_{R_{\text{tumor}}}/I_{B_{\text{tumor}}}}{I_{R_{\text{normal}}}/I_{B_{\text{normal}}}}. \quad (4)$$

2.2.4 Spectrophotometric analysis on normal CAM

Spectrophotometric analysis was carried out on normal CAM in order to verify the effect of PVP on HY uptake in normal tissue. Solutions with various HY concentrations (10 μM , 50 μM , and 100 μM) were preliminarily tested, and 100 μM was chosen as a fixed HY concentration, as it produced absorption signals that were satisfactorily strong and distinguishable for a spectrophotometer. The making of HY solutions and incubation of HY solutions on CAM followed the same protocol used in DFEI experiments stated earlier. Solutions of 0, 100- μM , 1-mM, and 5-mM PVP K29/32 solutions with 500- μM NMP were used for the delivery of HY. After 1-h incubation in the absence of light, the excessive HY solution (if any) remaining on the surface of normal CAM was collected. Each surface was washed once with 1-mL 0.9% w/v NaCl solution, and the volume of retrieved washing solution was measured to exclude the possibility of leaking CAM, since the leakage would largely affect the amount of HY retrieved. The CAM was then cut out, weighed, minced, sonicated with 1-mL ethanol on ice, and then centrifuged at 1200 rpm for 5 min at room temperature to remove precipitates. The absorbance of HY in the obtained supernatant was determined spectrophotometrically and divided by the weight of each CAM to produce HY uptake per unit weight of CAM. The calculation results from eggs treated with PVP solutions were normalized to those from eggs treated with non-PVP solutions for normalization purposes. The same treatment was applied on 5 to 7 eggs for each PVP concentration for the purpose of average calculation. Determination of HY uptake by excessive HY solution retrieved from CAM surface after incubation was avoided, as it was found that the solution had been adsorbed by the time of collection, and retrieving any remaining solution was practically impossible in most of the cases.

3 Results

3.1 FCS Analysis on HY Solutions

Many reports have demonstrated effects of viscosity on drug release and uptake processes.⁴³⁻⁴⁹ Therefore, when using FCS to test the interaction of HY and vinyl pyrrolidone polymers, a correction for viscosity is necessary. Both the increase of viscosity and interactions (if present) between HY and vinyl

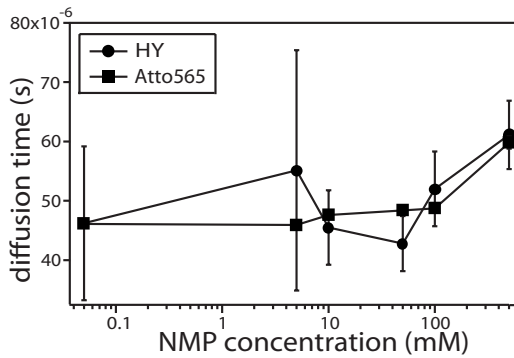


Fig. 2 Change in diffusion time with the concentration of NMP, with the error bars showing the standard deviation of each data point expressed as mean±S.D. Autocorrelation curves were fitted with 3-D one-particle model.

pyrrolidone polymers can contribute to the slowing down of the apparent diffusion rate of HY in solutions, which will be detected by FCS as compared to a solution where increased viscosity and molecule interaction are absent. To distinguish possible molecular interactions from increased viscosity that could result in false-positive FCS detection, Atto 565, a fluorophore, was used for correcting the changes in viscosity induced by elevations in NMP/PVP concentration. With a similar molecular weight to HY, Atto 565 is an ideal control for HY for such correction, as it also has similar excitation and emission spectra to HY that made the measurement possible under the same FCS-optimized settings (Table 1).

Measurements were first carried out on HY solutions with increasing NMP concentrations to disprove interaction between HY and NMP. The diffusion times of HY and Atto 565 from FCS assay on solutions with different concentrations of NMP showed a similar decrease of the diffusion coefficient of HY and Atto 565 in the more viscous solutions caused by the increase of NMP concentration (Fig. 2), indicating that any possible change in the diffusion pattern with a fixed concentration of NMP and the addition of vinyl pyrrolidone polymers will be solely due to vinyl pyrrolidone polymers rather than NMP. NMP was thus kept in the solution as a preliminary solvent for solution preparation as well as a penetration enhancer at a concentration of 5 mM.

With the addition of vinyl pyrrolidone polymers, widening of the autocorrelation curves of Atto 565 occurred due to the increase of viscosity (Fig. 1). Diffusion times of HY and Atto 565 with the presence of PVP K29/32, C15, and S630 at concentrations below 100 μM showed no statistically significant difference when the autocorrelation curves were fitted with a 3-D one-particle model [Eq. (1)]. With PVP concentrations above 100 μM (regardless of which type of PVP used), however, HY displayed significantly slower diffusion than Atto 565, resulting in wider autocorrelation curves compared to those of Atto 565. Fitted with a 3-D two-particle model [Eq. (2)], these autocorrelation curves of HY revealed changes in bound fractions (Fig. 3) and ratio of average number of HY particles over Atto 565 particles (R_N) within the focal volume (Fig. 4). A general trend of increase in the bound fraction occurred with increasing concentration of vinyl pyrrolidone polymers. At very high concentrations of the polymers (PVP K29/32 10 mM, C15 10 mM, and S630 7 mM), however,

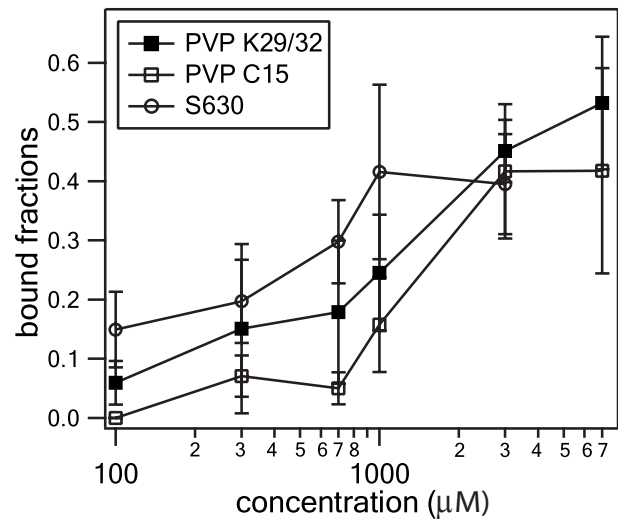


Fig. 3 Bound fractions of HY to cascading concentrations of PVP K29/32, C15, and S630 in 5-mM NMP solutions from FCS assay (3-D two-particle model).

intensive aggregation appeared, as shown by large intensity peaks during FCS measurements. Despite the change in refractive index of the solution as revealed by the rising of the average number of Atto 565 particles within the focal volume, R_N underwent an increase with concentration elevation for all three polymers. This finding indicated an increase of the number of HY particles in solution.

3.2 FLIM Measurements on HY Solutions

In order to further reveal the change in local environment and status of HY molecules with the addition of the vinyl pyrrolidone polymers in the formulation, FLIM measurements were performed on solutions with the same polymer concentrations as in the FCS experiments. DMSO solutions with equivalent monomer concentrations were used as a control for the

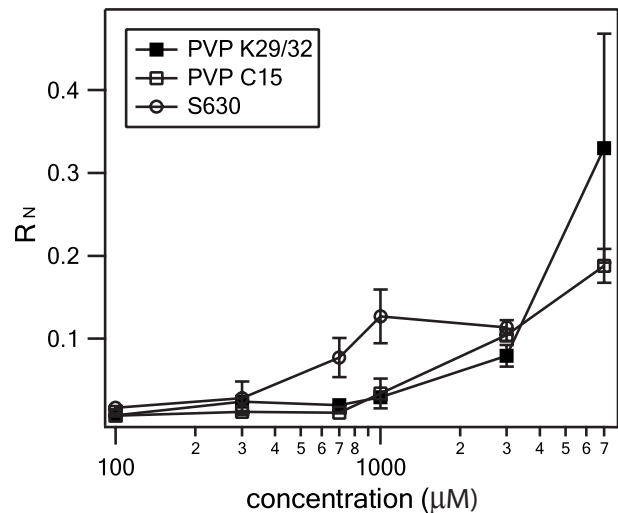


Fig. 4 Increasing ratio of numbers of HY/Atto 565 particles with cascading concentrations of PVP K29/32, C15, S630, and a fixed concentration of 5-mM NMP in solutions.

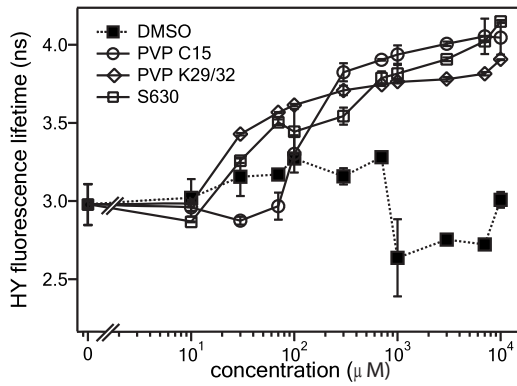


Fig. 5 HY fluorescence lifetime in solutions with a fixed concentration of 5-mM NMP and various concentrations of PVP K29/32, C15, S630, and DMSO in equivalent monomer concentrations.

change in hydrophobicity. With the addition of vinyl pyrrolidone polymers in solutions, the average fluorescence lifetime of HY displayed a general increase starting between the polymer concentration of 10 μM and 100 μM in all three cases, while the control measurements with increasing DMSO concentration showed no obvious trend (Fig. 5).

3.3 DFEI on Tumor-Implanted CAM

In order to further assess the effect of HY-PVP binding, CAM was adopted as the model membrane for implanting cultured MGH cells. DFEI was performed, and data were collected after 1-h and 3-h incubation with HY and PVP solutions. Images were processed, and statistical results from 6 to 8 eggs per group were plotted in Fig. 6. The tumor and normal tissue

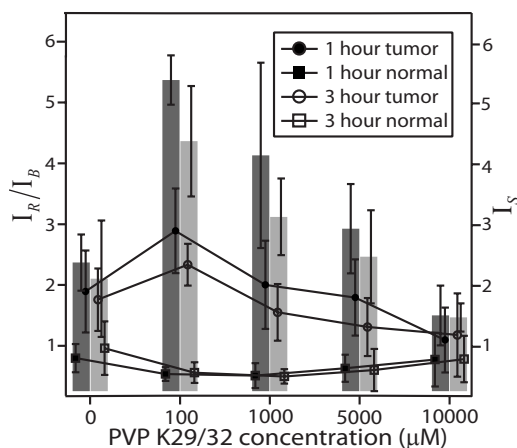


Fig. 6 Selectivity index I_s and the I_R/I_B ratios of both tumor and normal tissues after 1 h and 3 h incubation in the absence of light obtained from fluorescence endoscopic image processing. Dark columns: I_s after 1 h incubation. Light columns: I_s after 3 h incubation. Solid circles: I_R/I_B value of tumor after 1 h incubation. Solid squares: I_R/I_B value of normal tissue after 1 h incubation. Open circles: I_R/I_B value of tumor after 3 h incubation. Open squares: I_R/I_B value of normal tissue after 3 h incubation. All were treated with HY 10 μM solutions with various PVP K29/32 concentrations as indicated. Each data point represents statistical results from 6 to 8 individual tests. All the error bars show the standard deviation of each data point expressed as mean \pm S.D.

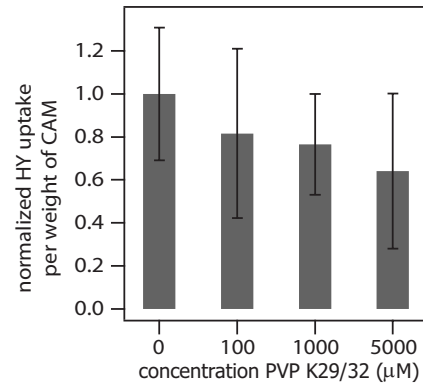


Fig. 7 Normalized HY uptake in normal tissues after 1 h incubation in the absence of light obtained from spectrophotometric analysis. Each data point represents statistical results from 6 to 8 individual tests. All the error bars show the standard deviation of each data point expressed as mean \pm S.D.

were better distinguished (higher HY uptake in tumor and lower HY uptake in normal tissue) with modest PVP concentrations (100 μM and 1 mM) in terms of I_s . The difference between tumor and normal tissue topped at 100 μM among the five PVP concentration groups and decreased with the rising of PVP concentration after 1 mM. Eggs treated with HY solutions with 100- μM , 1-mM, and 5-mM PVP showed a faster clearance reflected in the decreasing of I_R/I_B in tumor than those treated with HY solutions without PVP, while no obvious difference of such kind was observed in normal tissue across different concentration of PVP. The 10-mM data point was collected over 6 out of 13 eggs, while the other 7 eggs showed various extents of damage (obvious shrinkage or bleeding of the vessels, deterioration of the normal CAM, distortion of the tumor, and death of the embryo) to the CAM after incubation. The HY uptake in this group was even less than eggs treated with HY solutions without PVP, accompanied with the poorest uptake selectivity as well as clearance after 3-h incubation. The control groups treated with non-HY solutions showed that both the tumor and normal tissues appeared healthy with no physical damage after 1-h and 3-h incubation with PVP concentration no more than 5 mM. The non-HY/PVP 10-mM control group showed the same response (tissue damage) as that treated with HY 10 μM /PVP 10 mM solutions stated earlier.

3.4 Spectrophotometric Analysis on Normal CAM

In order to verify the effect of PVP on HY uptake in normal tissue, HY in normal CAM after 1-h incubation in the absence of light was extracted and was then subjected to spectrophotometric analysis. The amount of HY retrieved from harvested CAM with a chemical extraction method followed by spectrophotometric analysis and normalization (represented by normalized HY absorbance per unit weight of CAM) showed lower uptake of HY in CAM when PVP is present. (Figure 7; multiple comparison with ANOVA test: $F=1.21$, $p=0.336261$. Student's t-test between the non-PVP group and 5-mM PVP group returned $t=1.77967$, $p=0.108833$, so the two groups are considered different at a confidence level of

89.1%.) The HY/PVP 10-mM solution was not tested with this method since the irritation of CAM as observed earlier would make any result obtained unreliable.

4 Discussion

PVP is a common pharmaceutical excipient, a bioadhesive, stabilizer, and dispersion agent. The FCS measurements in this study revealed effects of viscosity and concentration of the excipient on the binding between a drug (HY) and PVP, which is important information when a drug delivery system is in its early formulation development stage.

The present study shows the potential of FCS being used for rapid preformulation screening of potential pharmaceutical excipients to identify their suitability and maximal concentration of the different pharmaceutical excipients before the actual testing for stability and efficacy of such preparations in either *in vitro* or *in vivo* system. The strength of interaction between the drug and the carrier system or formulation additives will determine whether the drug can be effectively released and made available for binding to the target site. When the adhesion between the carrier and the drug is stronger than the interaction between the drug and the target site of interest, the formulation will not be effective even though the drug could be very promising for a particular new indication. For example, if the drug is bound tightly to its carrier system and its interaction to the cellular membrane is weaker, the drug cannot be available to be transported across the cell membrane for its intracellular activity to occur. Together with confocal microscopy, this approach can help in understanding existing contradicting data regarding the uptake mechanism of certain drugs.

The interaction of HY with vinyl pyrrolidone polymers was either nonexistent or nonobservable by FCS measurements at concentrations below 100 μM . The trend of bound fractions indicated that more interactions between HY and the polymers occurred in all three cases when more molecules of the polymers were available in the environment. The concentrations of the three polymers, however, must not be too high, since massive aggregations were found to occur according to FCS observations, and large-sized aggregates are believed to have difficulties trafficking cellular membranes.

The disaggregation and solubilizing process of HY in aqueous solution with the help of increasing vinyl pyrrolidone polymers was proved by the increase of R_N . The trend indicates that the number of HY particles within the focal volume increased to a larger extent compared with the number of Atto 565 particles, which represents the increase in the focal volume. The obvious increase of HY particles with the addition of the polymers can only be due to the disaggregation and increased water solubility of HY. This finding of FCS agrees with the previous observation our group made with fluorescence intensity measurements.⁵⁰

The increase of average fluorescence lifetime of HY with increasing polymer concentration corroborated the observed increase of R_N from FCS measurements. We attribute the longer fluorescence lifetime of HY to the disaggregation and solubilizing effect of the polymers since the aggregated form of HY should exhibit shorter lifetimes due to self-quenching. A similar phenomenon of lifetime decrease has been reported in the case of accumulation and aggregation of HY in low-

density lipoprotein molecules⁵¹ as well as in cells.²¹ It should be noted that the lifetime is inversely proportional to the square of the refractive index, and thus an increase in refractive index due to an increase in the PVP concentration, as shown by the Atto565 experiments, would have suggested a lifetime decrease.⁵²⁻⁵⁵ However, in the case of HY, we find an increase of the lifetime with PVP concentration, despite the increase in refractive index.

Comparison of PDD effects on the tumor-implanted CAM model among HY solutions with various PVP concentrations showed improvement on HY uptake selectivity when PVP was present in modest concentrations (100 μM to 1 mM as the optimum concentration range). The differentiation from tumor to normal tissue displayed a decrease after 3-h incubation, mainly due to the clearance of HY from tumor while the level of HY in normal tissues remained unchanged. There are several possible reasons for the increased HY uptake by tumor and improved uptake selectivity. As indicated by the FCS results reported herein, a modest concentration of PVP in water solutions induces its binding with HY molecules (displayed as rising binding fractions with concentration) as well as HY disaggregation in water solutions (displayed as rising number of particles with concentration), both of which should be in favor of HY *in vivo* delivery with topical applications. On the other hand, an optimum uptake effect depends on the balance of hydrophilicity and lipophilicity of the delivery system, thus too much PVP (above 1 mM) might “reverse” the HY uptake since excessive PVP might also keep HY from the incorporation with and penetration into the lipid biomembrane. The decrease of HY uptake in normal tissue as indicated by the drop in I_R/I_B ratio with PVP at 1 mM and below does not necessarily imply any direct relationship of the addition of PVP and the change of HY uptake by normal tissue, because the implanted tumor could as well deprive the normal CAM tissue of HY, given that the HY uptake in tumors can be several times higher than that in normal tissues as observed in this experiment. Only with reliable evidence from statistics of HY uptake obtained from normal CAM with no tumor implanted can it be concluded that the addition of PVP is the direct reason for reduced normal tissue uptake of HY.

Thus, there was the need for spectrophotometric analysis to determine HY uptake by normal tissue. Compared with tissues treated with 100- μM HY/500- μM NMP solution, CAMs treated with the addition of 100- μM , 1-mM, or 5-mM PVP showed less HY uptake per unit weight of CAM. This phenomenon corroborates the lower HY fluorescence signal observed with DFEI in the normal region of tumor-implanted CAM. For all three PVP concentrations (100 μM , 1 mM, and 5 mM) tested, it is reasonable to believe that PVP had some sort of “protection” effect on normal CAM tissue against HY uptake.

The underlying scheme for the different effects of PVP on HY uptake by tumor and normal tissue to occur remains to be further explored. On one hand, the binding of HY with PVP might reduce the ability of HY to penetrate cellular membrane. On the other hand, the disaggregation and solubilizing effects offer more HY available for uptake. Both schemes are competing against each other, while the possibly different effects of PVP on tumor and normal cell membrane might add several other competitors to the whole picture. Therefore,

there is at the moment no suggested optimum concentration for PVP where full disaggregation of HY can be reached without possible reduction of HY availability by binding or tissue damage by high PVP concentration. HY in these cases is disaggregated to the extent enough to enhance HY action, while PVP concentration is low enough to avoid tissue damage.

In both FCS and FLIM measurements, the concentrations of PVP were the same (from 0 to 10 mM), and NMP was kept in the solution at a concentration of 5 mM. The HY concentrations, however, were different because of the principle of both techniques. Both FCS and FLIM indicated the disaggregation of HY with the help of PVP. In other words, the PVP concentrations used proved to be enough for the disaggregation of HY at different concentrations in both sets of measurements.

Concluding from the preceding, an addition of PVP into the drug transportation system can be in favor of HY PDD in terms of tumor selective uptake. Excessive concentration of PVP (e.g., 10 mM in solution), however, resulted in either very poor uptake selectivity as reflected by low differentiation in I_5 or massive destruction of both tumor and normal tissues represented by shrinkage or bleeding of the vessels, deterioration of the normal CAM, distortion of the tumor, and death of the embryo, among other effects. This phenomenon is not a response for HY treatment as proven by non-HY control groups. Thus, it could be partly due to the strong water absorption of PVP, which could deprive the tissues of water, or direct effects of PVP on the structure of the tissues.

5 Conclusion

The present study indicates the use of FCS and FLIM for testing of pharmaceutical preparations as demonstrated by the HY-NMP-PVP system. FCS can be used for efficient screening of molecular interactions in potential pharmaceutical formulations when an appropriate fluorophore with similar spectrum and molecular weight to the drug of interest is employed to correct the viscosity changes induced by the pharmaceutical excipients. FLIM can be used for understanding the change of environment and status of the molecules induced by the change in the formulation. The results obtained from FCS and FLIM measurements in HY solutions were further analyzed, and the HY-NMP-PVP system was investigated using the *in vivo* CAM model implanted with human bladder carcinoma cells. DFEI revealed that the molecular binding between HY and PVP as indicated by FCS results coordinates with the favored selective uptake by tumor tissues. Spectrophotometric analysis on the amount of HY in normal CAM showed lower HY uptake in normal tissue when PVP is present, corroborating the lower signal strength of HY in normal tissue in DFEI assay on tumor-implanted CAM. The study demonstrates the binding ability of excessive PVP to HY, which provides possible prevention against the passive uptake of HY by normal CAM tissue. Therefore, we suggest the potential of using the appropriate concentration of PVP in the HY delivery system to replace albumin as a solubilizer in clinical formulations, since PVP is considered highly biocompatible in a wide range of concentrations.

Acknowledgments

J. Liu is a recipient of a postgraduate scholarship from the National University of Singapore. She thanks Mr. William Chin for helpful discussion and Dr. Paul Wan Sia Heng from the Department of Pharmacy, National University of Singapore, for his generosity in supplying the excipients. T. Wohland gratefully acknowledges funding from the National University of Singapore, Grant No. R-143-000-338-112.

References

1. P. Schwille and E. Haustein, *Fluorescence Correlation Spectroscopy: An Introduction to Its Concepts and Applications*, Biophysics Textbooks Online (BTOL) (2004), www.biophysics.org/education/resources.htm.
2. E. L. Elson and D. Magde, "Fluorescence correlation spectroscopy. I. conceptual basis and theory," *Biopolymers* **13**, 1–27 (1974).
3. M. Ehrenberg and R. Rigler, "Rotational brownian motion and fluorescence intensity fluctuations," *Chem. Phys.* **4**(3), 390–401 (1974).
4. M. Ehrenberg and R. Rigler, "Fluorescence correlation spectroscopy applied to rotational diffusion of macromolecules," *Q. Rev. Biophys.* **9**(1), 69–81 (1976).
5. M. Kinjo and R. Rigler, "Ultrasensitive hybridization analysis using fluorescence correlation spectroscopy," *Nucleic Acids Res.* **23**(10), 1795–1799 (1995).
6. U. Meseth, T. Wohland, R. Rigler, and H. Vogel, "Resolution of fluorescence correlation measurements," *Biophys. J.* **76**(3), 1619–1631 (1999).
7. M. Auer, K. J. Moore, F. J. Meyer-Almes, R. Guenther, A. J. Pope, and K. A. Stoeckli, "Fluorescence correlation spectroscopy: lead discovery by miniaturized HTS," *Drug Discovery Today* **3**(10) 457–465 (1998).
8. K. J. Moore, S. Turconi, S. Ashman, M. Ruediger, U. Haupts, V. Emerick, and A. J. Pope, "Single molecule detection technologies in miniaturized high throughput screening: fluorescence correlation spectroscopy," *J. Biomol. Screening* **4**(6), 335–353 (1999).
9. L. Zemanova, A. Schenk, M. J. Valler, G. U. Nienhaus, and R. Heilker, "High-throughput screening of interactions between G protein-coupled receptors and ligands using confocal optics microscopy," *Methods Mol. Biol.* **305**, 365–383 (2005).
10. F. Delie, R. Gurny, and A. Zimmer, "Fluorescence correlation spectroscopy for the characterization of drug delivery systems," *Biol. Chem.* **382**(3), 487–490 (2001).
11. A. Periasami, M. Elangovan, H. Wallrabe, J. N. Demas, M. Barroso, D. L. Brautigan, and R. N. Day, *Methods in Cellular Imaging*, Oxford University Press, New York (2001).
12. B. Herman, *Fluorescence Microscopy*, 2nd ed., Springer-Verlag, New York (1998).
13. J. R. Lakowicz, *Principles of Fluorescence Spectroscopy*, 2nd ed., Kluwer Academic and Plenum Press, New York (1999).
14. A. Periasami and R. N. Day, "Visualizing protein interactions in living cells using digitized BFG imaging and FRET microscopy," in K. F. Sullivan and S. A. Key, Eds., *Methods in Cell Biology, Volume 58: Green Fluorescent Proteins*, Academic Press, New York (1999).
15. M. Elangovan, R. N. Day, and A. Periasami, "Nanosecond fluorescence resonance energy transfer—fluorescence lifetime imaging microscopy to localize the protein interactions in a single living cell," *J. Microsc.*, **205**(Pt 1) 3–14 (2002).
16. T. W. Gadella Jr. and T. M. Jovin, "Oligomerization of epidermal growth factor receptors on a431 cells studied by time-resolved fluorescence imaging microscopy. A stereochemical model for tyrosine kinase receptor activation," *J. Cell Biol.* **129**(6), 1543–1558 (1995).
17. F. Waharte, C. Spriet, and L. Heliot, "Setup and characterization of a multiphoton FLIM instrument for protein-protein interaction measurements in living cells," *Cytometry, Part A*, **69A**(4), 299–306 (2006).
18. T. Yamazaki, N. Ohta, I. Yamazaki, and P. S. Song, "Excited-state properties of hypericin: electronic spectra and fluorescence decay kinetics," *J. Phys. Chem.* **97**(30), 7870–7875 (1993).
19. F. Gai, M. J. Fehr, and J. W. Petrich, "Observation of excited-state tautomerization in the antiviral agent hypericin and identification of its fluorescent species," *J. Phys. Chem.* **98**(22), 5784–5795 (1994).
20. D. S. English, R. T. Doyle, J. W. Petrich, and P. G. Haydon, "Sub-

- cellular distributions and excited-state processes of hypericin in neurons," *Photochem. Photobiol.* **69**(3), 301–305 (1999).
21. P. Taroni, G. Valentini, D. Comelli, C. D'Andrea, R. Cubeddu, D. N. Hu, and J. E. Roberts, "Time-resolved microspectrofluorimetry and fluorescence lifetime imaging of hypericin in human retinal pigment epithelial cells," *Photochem. Photobiol.* **81**(3), 524–528 (2005).
 22. D. E. Dolmans, D. Fukumura, and R. K. Jain, "Photodynamic therapy for cancer," *Nat. Rev. Cancer* **3**(5), 380–387 (2003).
 23. H. G. Sim, W. K. O. Lau, M. Olivo, P. H. Tan, and C. W. S. Cheng, "Is photodynamic diagnosis using hypericin better than white-light cystoscopy for detecting superficial bladder carcinoma?," *Urban Land* **95**(9), 1215–1218 (2005).
 24. M. A. D'Hallewin, P. A. De Witte, E. Waelkens, W. Merlevede, and L. Baert, "Fluorescence detection of flat bladder carcinoma *in situ* after intravesical instillation of hypericin," *J. Urol. (Baltimore)* **164**(2), 349–351 (2000).
 25. W. W. L. Chin, W. K. O. Lau, C. L. L. Saw, K. W. Kho, and M. Olivo, "Photodynamic-induced vascular damage of the chick chorioallantoic membrane model using perylenequinones," *Int. J. Oncol.* **25**(4), 887–891 (2004).
 26. C. L. L. Saw, P. W. S. Heng, W. W. L. Chin, K. C. Soo, and M. Olivo, "Enhanced photodynamic activity of hypericin by penetration enhancer n-methyl pyrrolidone formulations in the chick chorioallantoic membrane model," *Cancer Lett.* **238**(1), 104–110 (2006).
 27. C. L. L. Saw, M. Olivo, W. W. L. Chin, K. C. Soo, and P. W. S. Heng, "Transport of hypericin across chick chorioallantoic membrane and photodynamic therapy vasculature assessment," *Biol. Pharm. Bull.* **28**(6), 1054–1060 (2005).
 28. C. L. L. Saw, M. Olivo, W. W. L. Chin, K. C. Soo, and P. W. S. Heng, "Superiority of n-methyl pyrrolidone over albumin with hypericin for fluorescence diagnosis of human bladder cancer cells implanted in the chick chorioallantoic membrane model," *J. Photochem. Photobiol., B* **86**(3), 207–218 (2007).
 29. C. L. L. Saw, M. Olivo, T. Wohland, C. Y. Fu, K. W. Kho, K. C. Soo, and P. W. S. Heng, "Effects of n-methyl pyrrolidone on the uptake of hypericin in human bladder carcinoma and co-staining with DAPI investigated by confocal microscopy," *Technol. Cancer Res. Treat.* **6**(5), 383–394 (2007).
 30. A. B. Uzdensky, D. E. Bragin, M. S. Kolosov, A. Kubin, H. G. Loew, and J. Moan, "Photodynamic effect of hypericin and a water-soluble derivative on isolated crayfish neuron and surrounding glial cells," *J. Photochem. Photobiol., B* **72**(1–3), 27–33 (2003).
 31. S. Sattler, U. Schaefer, W. Schneider, J. Hoelzl, and C. M. Lehr, "Binding, uptake, and transport of hypericin by caco-2 cell monolayers," *J. Pharm. Sci.* **86**(10), 1120–1126 (1997).
 32. A. R. Kamuhabwa, P. Agostinis, M. A. D'Hallewin, A. Kasran, and P. A. de Witte, "Photodynamic activity of hypericin in human urinary bladder carcinoma cells," *Physica D* **20**(4), 2579–2584 (2000).
 33. K. Das, A. V. Smirnov, J. Wen, P. Miskovsky, and J. W. Petrich, "Photophysics of hypericin and hypocrellin in a complex with subcellular components: interactions with human serum albumin," *Photochem. Photobiol.* **69**(6), 633–645 (1999).
 34. C. L. L. Saw, M. Olivo, K. C. Soo, and P. W. S. Heng, "Delivery of hypericin for photodynamic applications," *Cancer Lett.* **241**(1), 23–30 (2006).
 35. X. Pan, W. Foo, W. Lim, M. H. Y. Fok, P. Liu, H. Yu, I. Maruyama, and T. Wohland, "Multifunctional fluorescence correlation microscope for intracellular and microfluidic measurements," *Rev. Sci. Instrum.* **78**(5), 053711 (2007).
 36. D. Magde, E. L. Elson, and W. W. Webb, "Fluorescence correlation spectroscopy. II. an experimental realization," *Biopolymers* **13**(1), 29–61 (1974).
 37. S. R. Aragon and R. Pecora, "Fluorescence correlation spectroscopy as a probe of molecular dynamics," *J. Chem. Phys.* **64**(4), 1791–1803 (1976).
 38. S. Hell, G. Reiner, C. Cremer, and E. H. K. Stelzer, "Aberrations in confocal fluorescence microscopy induced by mismatches in refractive index," *J. Microsc.* **169**, 391–405 (1993).
 39. W. W. L. Chin, W. K. O. Lau, R. Bhuvaneshwari, P. W. S. Heng, and M. Olivo, "Chlorin e6-polyvinylpyrrolidone as a fluorescent marker for fluorescence diagnosis of human bladder cancer implanted on the chick chorioallantoic membrane model," *Cancer Lett.* **245**(1–2), 127–133 (2007).
 40. M. Richardson and G. Singh, "Observations on the use of the avian chorioallantoic membrane (CAM) model in investigations into angiogenesis," *Curr. Drug Targets Cardiovasc. Haematol. Disord.* **3**(2), 155–185 (2003).
 41. W. Zheng, M. Olivo, R. Sivanandan, P. Karuman, T. K. Lim, and K. C. Soo, "Endoscopy imaging of 5-ala-induced PPIX fluorescence for detecting early neoplasms in the oral cavity," *Proc. SPIE* **4597**, 128–132 (2001).
 42. D. Zaak, D. Frimberger, H. Stepp, S. Wagner, R. Baumgartner, P. Schneede, M. Siebels, R. Knuchel, M. Kriegmair, and A. Hofstetter, "Quantification of 5-aminolevulinic acid induced fluorescence improves the specificity of bladder cancer detection," *J. Urol. (Baltimore)* **166**(5), 1665–1669 (2001).
 43. J. S. Hao, L. W. Chan, Z. X. Shen, and P. W. S. Heng, "Complexation between PVP and Gantrez polymer and its effect on release and bioadhesive properties of the composite PVP/Gantrez films," *Pharm. Dev. Technol.* **9**(4), 379–386 (2004).
 44. L. W. Chan, T. W. Wong, P. C. Chua, P. York, and P. W. S. Heng, "Anti-tack action of polyvinylpyrrolidone on hydroxypropylmethylcellulose solution," *Chem. Pharm. Bull. (Tokyo)* **51**(2), 107–112 (2003).
 45. Y. T. Tan, K. K. Peh, and O. Al-Hanba, "Investigation of interpolymer complexation between carbopol and various grades of polyvinylpyrrolidone and effects on adhesion strength and swelling properties," *J. Pharm. Pharm. Sci.* **4**(1), 7–14 (2001).
 46. M. K. Chun, C. S. Cho, and H. K. Choi, "Mucoadhesive drug carrier based on interpolymer complex of poly(vinyl pyrrolidone) and poly(acrylic acid) prepared by template polymerization," *J. Controlled Release* **81**(3), 327–334 (2002).
 47. J. Kuntsche, K. Westesen, M. Drechsler, M. H. J. Koch, and H. Bunjes, "Supercooled smectic nanoparticles, a potential novel carrier system for poorly water soluble drugs," *Pharm. Res.* **21**(10), 1834–1843 (2004).
 48. P. Suhonen, T. Jarvinen, K. Lehmusaaari, T. Reunamaki, and A. Urtili, "Ocular absorption and irritation of pilocarpine prodrug is modified with buffer, polymer, and cyclodextrin in the eyedrop," *Pharm. Res.* **12**(4), 529–533 (1995).
 49. D. S. Jones, M. S. Lawlor, and A. D. Woolfson, "Rheological and mucoadhesive characterization of polymeric systems composed of poly(methylvinylether-co-maleic anhydride) and poly(vinylpyrrolidone), designed as platforms for topical drug delivery," *J. Pharm. Sci.* **92**(5), 995–1007 (2003).
 50. C. L. L. Saw, M. Olivo, K. C. Soo, and P. W. S. Heng, "Spectroscopic characterization and photobleaching kinetics of hypericin-N-methyl pyrrolidone formulations," *Photochem. Photobiol. Sci.* **5**(11), 1018–1023 (2006).
 51. P. Mukherjee, R. Adhikary, M. Halder, J. W. Petrich, and P. Miskovsky, "Accumulation and interaction of hypericin in low-density lipoprotein—a photophysical study," *Photochem. Photobiol.* **84**(3), 706–712 (2008).
 52. S. J. Strickler and R. A. Berg, "Relationship between absorption intensity and fluorescence lifetime of molecules," *J. Chem. Phys.* **37**(4), 814–822 (1962).
 53. D. Toptygin, R. S. Savtchenko, N. D. Meadow, S. Roseman, and L. Brand, "Effect of the solvent refractive index on the excited-state lifetime of a single tryptophan residue in a protein," *J. Phys. Chem. B* **106**(14), 3724–3734 (2002).
 54. K. Suhling, J. Siegel, D. Phillips, P. M. W. French, S. Leveque-Fort, S. E. D. Webb, and D. M. Davis, "Imaging the environment of green fluorescent protein," *Biophys. J.* **83**(6), 3589–3595 (2002).
 55. J. W. Borst, M. A. Hink, A. van Hoek, and A. J. W. G. Visser, "Effects of refractive index and viscosity on fluorescence and anisotropy decays of enhanced cyan and yellow fluorescent proteins," *J. Fluoresc.* **15**(2) 153–160 (2005).